Review Article

Characterization of coronary atherosclerosis by intravascular imaging modalities

Satoshi Honda[1,2], Yu Kataoka[1], Tomoaki Kanaya[1], Teruo Noguchi[1], Hisao Ogawa[1,3], Satoshi Yasuda[1,2]

[1]Department of Cardiovascular Medicine, National Cerebral and Cardiovascular Center, Suita, Japan; [2]Department of Advanced Cardiovascular Medicine, [3]Department of Cardiovascular Medicine, Graduated School of Medical Science, Kumamoto University, Kumamoto, Japan

Contributions: (I) Conception and design: Y Kataoka, S Honda; (II) Administrative support: None; (III) Provision of study materials or patients: Y Kataoka, S Honda, T Kanaya; (IV) Collection and assembly of data: Y Kataoka, S Honda; (V) Data analysis and interpretation: None; (VI) Manuscript writing: All authors; (VII) Final approval of manuscript: All authors.

Correspondence to: Yu Kataoka, MD. Department of Cardiovascular Medicine, National Cerebral and Cardiovascular Center, 5-7-1, Fujishirodai, Suita, Osaka, Japan. Email: yu.kataoka@ncvc.go.jp.

Abstract: Coronary artery disease (CAD) is highly prevalent in Western countries and is associated with morbidity, mortality, and a significant economic burden. Despite the development of anti-atherosclerotic medical therapies, many patients still continue to suffer from coronary events. This residual risk indicates the need for better risk stratification and additional therapies to achieve more reductions in cardiovascular risk. Recent advances in imaging modalities have contributed to visualizing atherosclerotic plaques and defining lesion characteristics *in vivo*. This innovation has been applied to refining revascularization procedure, assessment of anti-atherosclerotic drug efficacy and the detection of high-risk plaques. As such, intravascular imaging plays an important role in further improvement of cardiovascular outcomes in patients with CAD. The current article reviews available intravascular imaging modalities with regard to its method, advantage and disadvantage.

Keywords: Atherosclerosis; plaque; imaging

Submitted Aug 31, 2015. Accepted for publication Oct 23, 2015.
doi: 10.21037/cdt.2015.12.05
View this article at: http://dx.doi.org/10.21037/cdt.2015.12.05

Introduction

Atherosclerosis is the main cause of coronary artery disease (CAD). Atherosclerosis is developed and promoted by mainly the influx of LDL particles and the production of inflammatory cytokines in the arterial wall (1). These atherogenic mechanisms build non-obstacle atherosclerotic plaques in its early stage. Majority of plaques remain quiescent, whereas some plaques progress and others suddenly cause its rupture, leading to the acute coronary events (2). Therapeutic modulation of atherogenic targets is a key for the prevention of CAD. Numerous large-scale clinical trials have demonstrated anti-atherosclerotic effects of 3-hydroxy-3-methylglutaryl coenzyme A reductase inhibitors or statins for the primary and secondary prevention (3-6). Statin has the ability to reduce atherosclerotic cardiovascular events and attenuate disease progression. In addition, high-intensity statin has the potential to regress coronary atheroma in patients with CAD (5,7,8). Despite these favorable effects of a statin, many patients still continue to develop cardiovascular events (9,10). This ongoing disease risk presents a considerable challenge suggesting the need to identify additional key therapeutic targets, and develop more effective forms of risk prediction and preventive therapies.

Coronary angiography (CAG) has been widely used for the diagnosis and quantification of obstructive stenosis in the clinical settings. CAG has enabled to characterize culprit plaques associated with CAD, assess acute and chronic vascular response after revascularization strategies, and investigate the effect of medical therapies. While CAG is still a gold standard for the evaluation of coronary

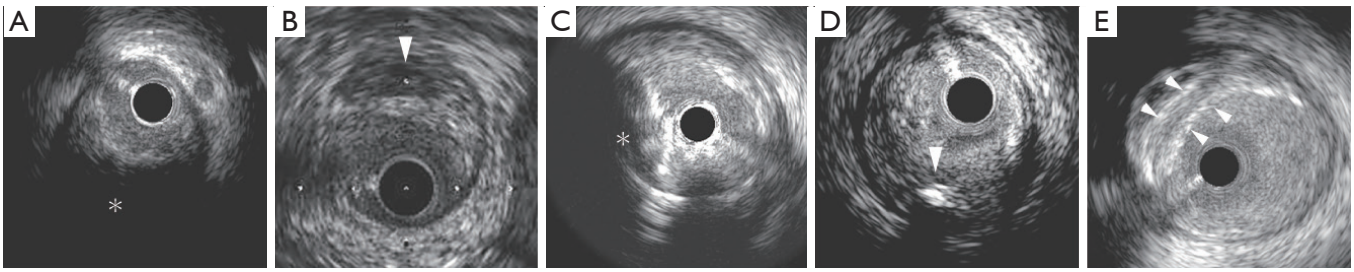

Figure 1 Plaque phenotypes on gray-scale IVUS. (A) Attenuated plaque: attenuation (asterisk) is observed between 3 to 9 o'clock; (B) echolucent plaque: arrow head indicates echolucent zone in the plaque; (C) calcified nodule: calcified nodule (asterisk) is observed as protrusion of calcified plaque with irregular luminal surface; (D) spotty calcification: arrow indicates small deposit of calcium in the plaque; (E) multiple layer appearance: double arrow heads indicate different layer of the plaque. IVUS, intravascular ultrasound.

artery stenosis, several limitations of CAG are recognized. CAG generates a 2-D silhouette of the arterial lumen and does not image the vessel wall, the site at which plaque accumulates. This disadvantage of CAG has stimulated the need to develop imaging modalities which enable to directly visualize plaques in the vessel wall.

Recent technological advances permit direct visualization of the full burden of coronary atherosclerosis. Intravascular imaging is increasingly becoming an important role in the evaluation of revascularization procedure but also in the assessment of drug efficacy. In addition, intravascular imaging has contributed to the identification of high-risk plaques that are likely to cause future cardiovascular events, so called "vulnerable plaques" (11,12). In this article, we summarize currently available intravascular imaging modalities to elucidate pathophysiology and characteristics of coronary atheroma *in vivo*.

Grayscale intravascular ultrasound (IVUS)

Grayscale IVUS uses miniaturized crystals which generate high-resolution, cross-sectional images of the vessel wall and lumen. Axial resolution is approximately 150 μm and the lateral resolution 300 μm. Grayscale IVUS allows robust quantitative measurements including lumen, vessel, and plaque area (13). Furthermore, Grayscale IVUS imaging enables to assess procedural outcomes after percutaneous coronary intervention (PCI). PCI with the guidance of grayscale IVUS has been demonstrated to reduce incidence of restenosis, stent thrombosis and cardiovascular events after PCI compared to angiographic guidance (14-17). Recently, IVUS has been increasingly used as the gold standard to evaluate natural history of coronary atherosclerosis under medical therapies (3,5,18-20).

Plaque phenotypes on grayscale IVUS

Based on echogenicity, plaques are classified in four categories by grayscale IVUS: soft plaque showing lesion echogenicity less than the surrounding adventitia, fibrous plaque with intermediate echogenicity between soft plaque and highly echogenic calcified plaques, calcified plaque having higher echogenicity than the adventitia with acoustic shadow, and mixed plaque (21). In addition to these grayscale IVUS-derived classifications of atherosclerotic plaques, distinct plaque phenotypes have been reported as follows.

Attenuated plaque

Attenuated plaque is defined as hypoechoic plaque with deep ultrasound attenuation without calcification or very dense fibrous plaque (*Figure 1A*). Histologically, attenuated plaques on IVUS correlate with a fibroatheroma containing large necrotic core or pathological intimal thickening (PIT) with a large lipid pool (22). Attenuated plaque is frequently observed at culprit lesion in patients with acute coronary syndrome (ACS) and is associated with deterioration of coronary flow and periprocedural myocardial infarction following PCI (23-25).

Echolucent plaque

Echolucent plaque is a lesion containing an intraplaque zone of absent or low echogenicity (*Figure 1B*) (26-28). Echolucent plaque is generally the result of high lipid content in a fibroatheroma, but relatively smaller size of necrotic core or lipid pool compared with attenuated plaque (22,29). This plaque phenotype has been shown as a signature of culprit lesions in patients with acute myocardial infarction (30).

Calcified nodule

Calcified nodule is a plaque phenotype associated with acute coronary events (31). Histologically, calcified nodule consists of fibrocalcific plaque with little or no underlying necrotic core, luminal surface that is disrupted by nodules of dense calcium, and overlying thrombus (32). Recent studies have validated features of calcified nodule on grayscale IVUS by comparing to pathological data in autopsy (33). Histopathological analyses have shown a distinct calcification with an irregular, protruding and convex luminal surface as grayscale-IVUS derived calcified nodule (*Figure 1C*). While this plaque feature is considered to associate with ACS, a sub-analysis of the PROSCPET study reported that patients with calcified nodule were less likely to develop major adverse cardiovascular events (34). Further investigation is warranted to elucidate clinical significance of calcified nodule on IVUS.

Spotty calcification

While extensive calcified lesions are generally considered to be clinically quiescent, scattered calcium pattern (spotty calcification) is associated with acute coronary events. Pathohistological study has shown the presence of small amount of calcium at high-risk lesions causing ACS or sudden cardiac death (35,36). Ehara *et al.* has demonstrated the presence of spotty calcification at culprit lesions in patients with acute coronary events *in vivo* (37). The definition of spotty calcification on IVUS is a lesion harboring only small calcium deposits with an arc of calcification of <90 (*Figure 1D*). Serial grayscale IVUS imaging has elucidated an accelerated plaque progression in patients with spotty calcification (38). As such, this calcium pattern on grayscale IVUS seems to be quite active and progressive form of disease.

Multiple layer appearance

Matsuo *et al.* has reported multiple layer appearance on grayscale IVUS as a high-risk feature of disease in heart transplant recipients (39). This phenotype exhibits multiple layers with distinct echogenicity (*Figure 1E*). In a serial grayscale IVUS study analyzing 132 heart transplant recipients, multiple layer appearance was associated with plaque progression. This might indicate the contribution of repeated episode of mural thrombosis to disease progression in heart transplant recipients.

Limitations of grayscale IVUS

Grayscale IVUS is an invasive procedure and is therefore currently limited to the assessment of patients who require CAG for a clinical indication. Conventional IVUS provides a suboptimal characterization of the composition of atherosclerotic plaque.

Virtual histology intravascular ultrasound (VH-IVUS)

While grayscale IVUS has the limited ability to analyze components within atherosclerotic lesions, VH-IVUS enables a detailed analysis of plaque composition. An advanced radiofrequency (RF) analysis of reflected ultrasound signals in a frequency domain analysis is used to visualize a reconstructed color-coded tissue map of plaque composition including fibrous, fibrofatty, necrotic core and dense calcium. The VH-IVUS algorithm has been validated against histology in autopsy specimens and in patients who underwent PCI. A high accuracy in detecting fibrous, fibrofatty, necrotic cores and calcium (autopsy: 79.7%, 81.2%, 85.5%, 92.8%, patients treated with PCI: 87.1%, 87.1%, 88.3%, 96.5%) has been already reported (40,41).

Plaque classifications by VH-IVUS

Currently, VH-IVUS classifies plaques into the following types.

Pathological intimal thickening (PIT)

PIT is considered as a progressive lesion in the early stages of atherosclerosis and represents a precursor lesion to fibroatheroma (31,42). It consists of mainly a mixture of fibrotic tissue and fibrofatty plaque with less than 10% each confluent necrotic core and dense calcium, respectively (*Figure 2A*) (44).

Thin-cap fibroatheroma (TCFA)

TCFA has been considered as a high-risk lesion causing acute coronary events (36,45). Histologically, TCFA is characterized by thin cap overlying a large necrotic core containing numerous cholesterol clefts (31). On VH-IVUS imaging, TCFA is characterized as a lesion having more than 10% confluent necrotic core with above 30 degree necrotic core abutting the lumen in at least three consecutive frames (*Figure 2B*) (44).

Thick-cap fibroatheroma (ThCFA)

ThCFA harbors a large lipid-necrotic core comprising large amount of extracellular lipid, cholesterol crystals, and necrotic

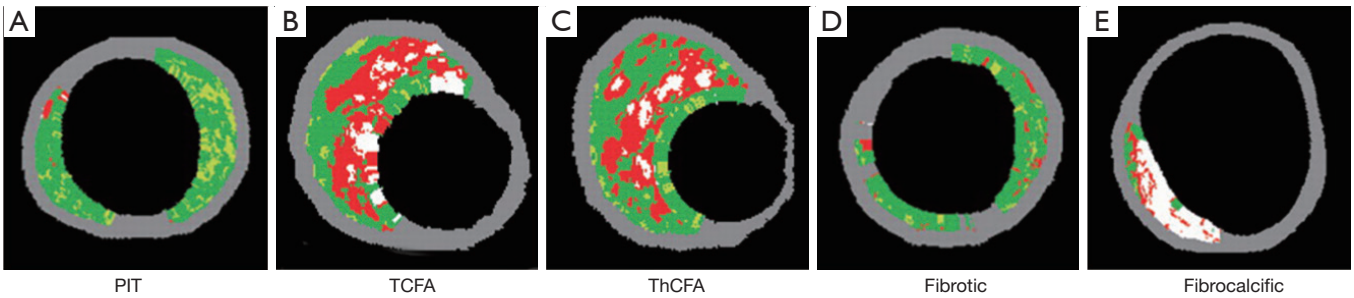

Figure 2 Virtual histology intravascular ultrasound (VH-IVUS) derived classification of plaques. (A) Pathological intimal thickening (PIT); (B) thin-cap fibroatheroma (TCFA); (C) thick-cap fibroatheroma (ThCFA); (D) fibrotic plaque; (E) fibrocalcific plaque. VH-IVUS, virtual histology intravascular ultrasound. Reproduce from: Garcia *et al*. Eur Heart J 2010;3:2456-69. (43).

debris, surrounded by a thick fibrous cap (44). The definition of ThCFA is a lesion with more than 10% confluent necrotic core and a definable fibrous cap (*Figure 2C*).

Fibrotic plaque

VH-IVUS derived fibrotic plaque is mainly fibrous tissue without confluent necrotic core or calcium (*Figure 2D*) (44). Fibrotic plaque is different from PIT with regard to the presence of fibro-fatty tissue. Fibrotic plaque contains few fibro-fatty tissue (<15%), whereas PIT contains >15% fibro-fatty tissue.

Fibrocalcific plaque

Fibrocalcific plaque is a collagen-rich lesion with nearly all fibrotic tissue and dense calcium with less than 10% confluent necrotic core (*Figure 2E*) (44).

Limitations of VH-IVUS

Identification of intraluminal organizing thrombus is currently not possible by RF analysis. The acquisition of VH-IVUS images is gated at the Rwave of the electrocardiography signal, which fails to allow to evaluate corresponding images in serial VH-IVUS imaging. Recent study raises questions about the accuracy of VH-IVUS to identify necrotic core. VH-IVUS-identified necrotic core was not correlated to histology in a swine atherosclerosis model (46). However, it is important to note that swine necrotic core is inherently different from human ones.

Integrated backscatter intravascular ultrasound (IB-IVUS)

IB-IVUS is another technique for tissue characterization of plaques. IB-IVUS analyzes RF-signals by applying a fast Fourier transformation of the frequency components of the backscattered signals, thereby calculating the intensity of the signal measured in decibels (dB). Different tissue components exhibit the different RF-signals, which enable to differentiate various plaque components. IB-IVUS classifies plaque components into 4 categories; fibrous (green), dense fibrosis (yellow), lipid pool (blue and purple) and calcification (red) (*Figure 3*). The sensitivity of IB-IVUS for calcification, fibrous and lipid-rich plaque was 100%, 94% and 84%, respectively on pathohistological analysis (47).

Limitation of IB-IVUS is that this modality is not sufficiently sensitive to distinguish intimal hyperplasia from lipid pool due to its similar IB values. While this imaging is validated by autopsy studies, studies using IB-IVUS are limited compared to grayscale IVUS and VH-IVUS. Further investigation is warranted to clarify the accuracy and usefulness of IB-IVUS in the clinical settings.

iMAP-IVUS

The iMAP-IVUS also acquires RF data continuously and then classifies plaques into four categories based on a spectra pattern; fibrous, fibrofatty, calcium, and necrotic core. *Ex vivo* validation study demonstrated accuracies for the detection of fibrous, lipidic, calcium and necrotic core as 95%, 98%, 98% and 97%, respectively (48). However, role and significance of iMAP imaging has not been fully investigated and established yet.

Optical coherence tomography (OCT)

OCT is a novel intravascular imaging modality using near-infrared light (1,300 nm). Compared to IVUS, OCT

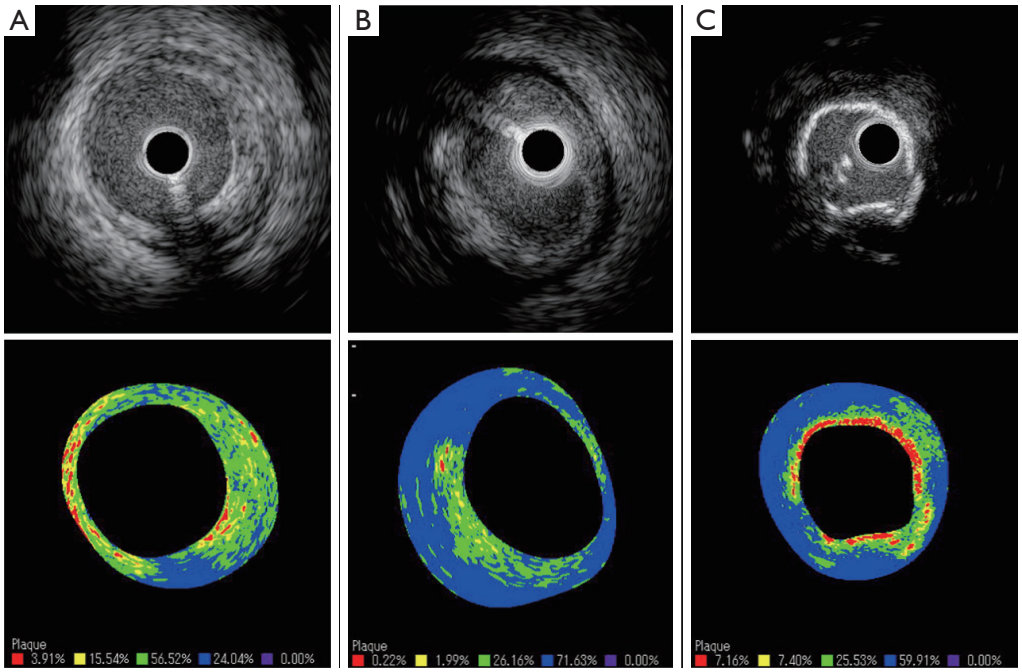

Figure 3 Images of plaque phenotype on IB-IVUS. Upper panels show grayscale IVUS images while lower panels show corresponding IB-IVUS images. (A) Fibrous plaque; grayscale IVUS shows high echogenic plaque between 12 to 8 o'clock. IB-IVUS image shows that most of plaque is classified into fibrous tissue (green and yellow); (B) lipid-rich plaque: graysclae IVUS image shows attenuated plaque between 6 to 12 o'clock. IB-IVUS image shows that most of plaque is classified into lipid-rich tissue (blue); (C) calcification: grayscale IVUS shows superficial entire-circumference of calcification. Corresponding IB-IVUS image indicates the presence of superficial calcification (red). IB-IVUS, integrated backscatter intravascular ultrasound. IVUS, intravascular ultrasound.

provides images of *in vivo* plaques with approximately 10 times higher resolution which is up to 10 μm in an axial resolution and to 20 μm in a lateral resolution. Since OCT has shallow penetration depth of imaging, this modality is superior to monitor plaque microstructures below the endothelial surface.

Plaque composition on OCT imaging

Fibrous plaque

A fibrous plaque exhibits high backscattering and a relatively homogeneous OCT signals (*Figure 4A*).

Lipid plaques

Lipid plaque is a signal-poor region with poorly delineated borders, a fast OCT signal drop-off, and little or no OCT signal backscattering (*Figure 4B*).

Calcified plaques

Calcification appears as a signal-poor or heterogeneous region with a sharply delineated border (*Figure 4C*).

Plaque microstructures

Thin fibrous cap

Fibrous cap on OCT is visualized as a signal-rich layer from the coronary artery lumen to the inner border of the underlying lipid-rich plaque. Thin fibrous cap is generally defined as fibrous cap <65 μm. A good correlation of the fibrous cap thickness between OCT image and histology has been reported (r=0.9, P<0.001) (49).

Thin-cap fibroatheroma (TCFA)

TCFA is an important feature of vulnerable plaque. While IVUS does not have enough abilities to visualize TCFA due to its limited spatial resolution, the high resolution of OCT enables to identify TCFA *in vivo*. OCT derived TCFA is characterized as the presence of thin fibrous cap (<65 μm) overlying a signal-poor lesion with diffuse border (lipid arc >90°) (*Figure 4D*).

Macrophage

Heavily infiltrated macrophage in thin fibrous cap is considered as a signature of vulnerable plaque (50). OCT

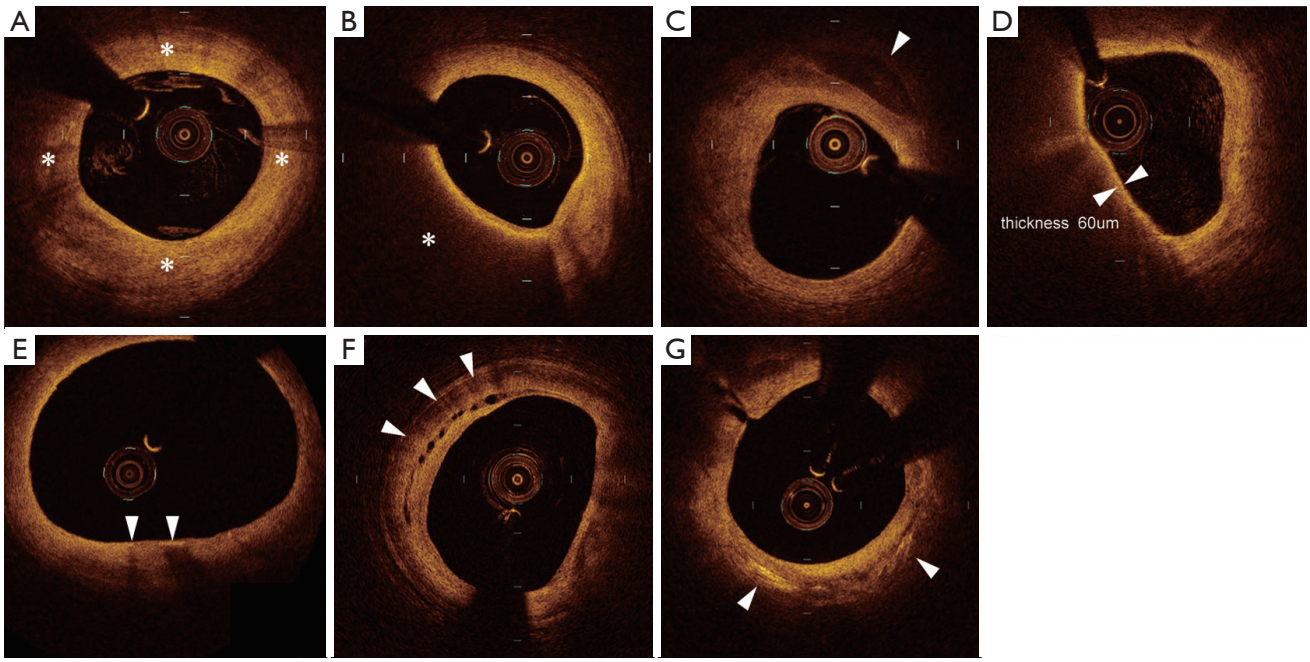

Figure 4 Images of plaque phenotype on OCT. (A) Fibrous plaque: fibrous plaque (asterisk) is imaged as a high backscattering and homogeneous region; (B) lipid-rich plaque: lipid-rich plaque (asterisk) is imaged as a signal-poor region with a poorly delineated borders; (C) fibrocalcific plaque: calcification (arrow head) is imaged by OCT from 12 to 3 o'clock, as well-delineated, signal-poor region; (D) fibrous cap: a fibrous cap (double arrow) is imaged as a signal-rich homogeneous region overlying a lipid core; (E) macrophage: macrophages (arrow heads) are imaged as signal-rich linear regions accompanied by high attenuation; (F) microchannel: microchannels (arrow heads) are imaged as signal poor voids observed in multiple contiguous frames; (G) cholesterol crystal: cholesterol crystal (arrows) is imaged by OCT as linear, high-backscattering structures within the plaque. OCT, optical coherence tomography.

visualizes macrophage accumulation as linear high-intensity signal on plaque surfaces with high attenuation (*Figure 4E*).

Microchannel

Microchannel is non-signal tubuloluminal structures without a connection to the vessel lumen and can usually be followed in multiple contiguous frames (*Figure 4F*). The presence of microchannel on OCT imaging has been shown to associate with a higher incidence of TCFA and future plaque progression (51,52).

Cholesterol crystal

Cholesterol crystal is defined as thin, linear region of high signal intensity within the lipid plaques (*Figure 4G*). The presence of cholesterol crystal is associated with enhanced plaque instability in patients with CAD (53).

In-stent neoatherosclerosis

In-stent neoatherosclerosis is newly formed atherosclerotic form within the neointimal tissue of stented segments. Emerging evidence suggests chronic inflammation and/or incompetent endothelium as important contributors to this pathological change within stent (54,55). Recent studies demonstrated that neoatherosclerosis could be developed in late phase after both bare metal stent (BMS) and drug-eluting stent (DES) implantation (56,57). In addition, earlier and more frequent development of neoatherosclerosis after DES implantation has been observed in pathohistological and clinical studies (58,59). Currently, neoatherosclerosis is considered as one of important mechanisms associated with late stent thrombosis and restenosis (54,57,60,61). OCT has a great potential to evaluate in-stent neoatherosclerosis *in vivo*. In-stent neoatherosclerosis by OCT imaging has been defined as the combination of neointimal diffuse thickening with intimal lipid-laden (poor signal region with diffuse borders) and the presence of fibrous cap (57,61,62). In a recent study analyzing in-stent restenosis lesions after DES implantation by OCT, TCFA and neointimal rupture within stent were observed in 52% and 58% of study

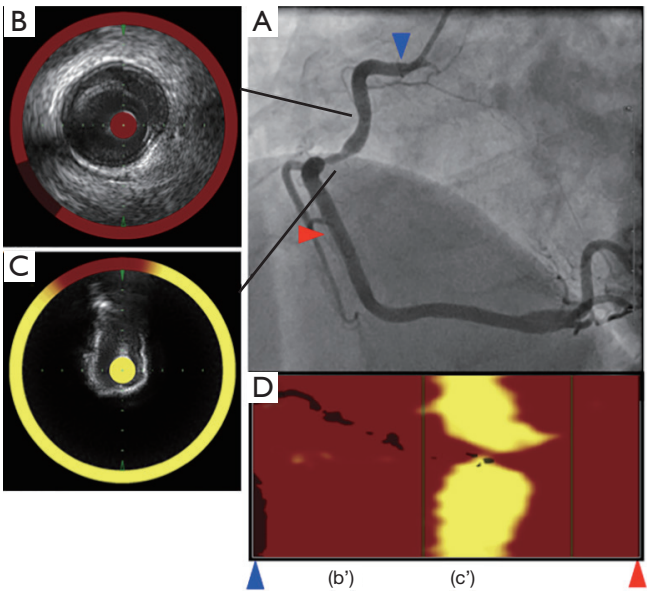

Figure 5 Lipid core plaque in the right coronary artery detected by NIRS-IVUS. (A) Angiography showed stenosis in the mid-right coronary artery. Automated pullback was performed from mid (red arrow head) to proximal right coronary artery (blue arrow head); (B) IVUS image shows plaque between 9 to 4 o'clock. The ring around the IVUS image represents the NIRS values. High probability of lipid core plaque is displayed as yellow and low probability as red. At this lesion, NIRS indicated no lipid core plaque; (C) the cross sectional IVUS image shows with superficial calcification and resultant shadowing in the mid-right coronary artery. NIRS showed nearly circumferential lipid core plaque; (D) this figure shows "chemogram" of the right coronary artery between red arrow head and blue arrow head. (B') Corresponds to *Figure 5B* lesion, while (C') corresponds *Figure 5C* lesion. NIRS, near infrared spectroscopy; IVUS, intravascular ultrasound.

subjects, respectively (57).

Limitations of OCT

Limitations of OCT are poor tissue penetration and interference from blood. OCT has a penetration depth of 2 to 3 mm, which prohibits imaging beyond the internal elastic lamina. Due to this limited penetration, it is difficult to evaluate the entire amount of plaques. This imaging is not suitable for visualizing atherosclerotic plaques in large arteries. Infusion of contrast medium is required during OCT imaging because infrared light does not penetrate red blood cells. This feature makes it difficult to use this imaging in patients with kidney disease.

Near-infrared spectroscopy (NIRS)

Spectroscopy is the measurement of the electromagnetic spectrum through interaction of light with molecules. Based on this method, NIRS imaging within coronary artery allows for the chemical characterization of biological tissues and can be used to assess lipid and protein content in atherosclerotic plaques. In an experimental animal study and *ex vivo* validation studies, this modality was shown to accurately detect the lipid content within atherosclerotic plaques (63-65). The sensitivity and specificity to detect lipid component was 90% and 93%, respectively. Recently, catheter-based NIRS imaging system has been developed (InfraReDx, Burlington, Massachusetts, USA). This device incorporates the rotating core with optical fibers which emit and absorb near-infrared light. NIR spectrometer delivers the light into a sample and then evaluates the proportion of light which is returned over the range of optical wavelength. After the NIRS system produces a spectrum through diffuse reflectance signal from an object, it displays a chemogram which corresponds to the lipid content (*Figure 5*).

Identification of high-risk plaques on NIRS

One recent study has investigated plaque features at culprit and non-culprit segments in patients with ST elevation myocardial infarction and autopsy segments without any lipid plaques (66). Culprit segments were more likely to exhibit a larger lipid core burden index (LCBI) compared to non-culprit segments (median LCBI; 523 *vs.* 90, P<0.001) and coronary autopsy lipid-free segments (median LCBI; 523 *vs.* 6, P<0.001). In addition, LCBI above 400 was an optimal cut-off to distinguish culprit segments in patients with ST elevation myocardial infarction from coronary specimens free of lipid component. Another study elucidated better evaluation of plaque characterization under the combination of NIRS and grayscale IVUS (29). In this study analyzing 131 lesions, attenuated (P<0.0001) and echolucent plaques (P=0.008) on grayscale IVUS were associated with a larger LCBI compared to calcified and non-calcified plaques. Another study demonstrated the utility of adding NIRS to conventional IVUS for the detection of fibroatheroma in the 116 coronary arteries from autopsy hearts (67). There were significant trends of increasing plaque burden and LCBI across more complex atheroma. Furthermore, adding NIRS derived-LCBI to the grayscale IVUS-derived plaque burden was significantly improved fibroatheroma detection accuracy. NIRS also has

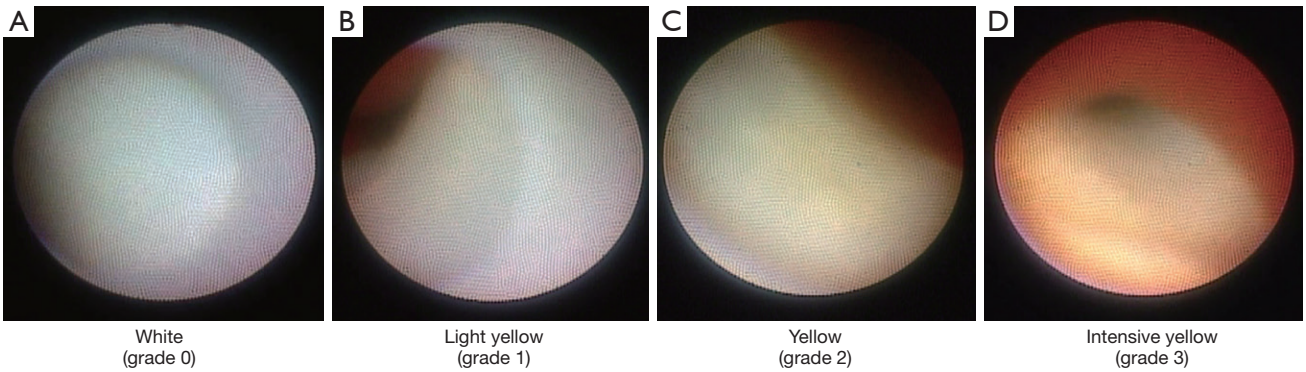

Figure 6 Classification of plaques by the yellowness of plaques on angioscopy image. Coronary plaques are classified by angioscopy according to the yellowness as follows: grade 0 = white; grade 1 = light yellow; grade 2 = yellow; grade 3 = intensive yellow.

the ability to predict periprocedural myocardial infarction following PCI (68). Goldstein *et al.* has reported that lesions with LCBI >500 were more likely to experience periprocedural myocardial infarction (P=0.0002) (69). These observations suggest the potential of NIRS imaging for the risk stratification of future coronary events and the management of revascularization procedure.

Limitations of NIRS imaging

NIRS is not able to evaluate the depth of lipid core and the volume of lipid quantitatively. In addition, current NIRS system does not have capabilities to evaluate other features of vulnerable plaque such as thin fibrous cap, macrophage infiltration. Further advances may permit detection of other plaque features implicated in vulnerability.

Coronary angioscopy

Intracoronary coronary angioscopy has the capability of direct visualization of the surface of the plaque through fiber optics *in vivo* with high resolution (<150 μm).

Visualized plaque features by coronary angioscopy

The advantage of coronary angioscopy is to assess plaque color and surface characteristics. Plaque color can be graded as white, light yellow, yellow or intensive yellow by coronary angioscopy (*Figure 6*). White plaques on coronary angioscopy correlate with mainly fibrous plaque, whereas yellow plaques have been shown to harbor lipid rich tissue or necrotic core. The intensity of yellow color is associated with its instability, and high yellow intensity of plaques has been reported to exhibit thin, fibrous caps overlying a lipid core (70-72). Morphology of plaques is also evaluable by coronary angioscopy. Stable plaque is lesion with smooth surface, whereas complex plaque exhibits an irregular surface. Ruptured plaque, eroded plaque, intimal flap, fissure and ulceration are another complex lesions identified by coronary angioscopy (73). This modality has the ability to clearly visualize thrombus, which is a coalescent red or white mass, or both, adhering to the intima or protruding into the inner lumen (74). On histological validation, while the sensitivity of grayscale IVUS for the detection of thrombus was only 57%, its sensitivity was 100% under angioscopy imaging (73).

Limitations of angioscopy

There are some limitations of coronary angioscopy. Firstly, it is difficult to conduct quantitative analysis of plaques with regard to color and volume. Second, coronary angioscopy images only surface of the coronary lumen. It requires displacement of blood within coronary arteries by injecting saline continuously.

Potential links between imaging features and the corresponding cardiovascular risk

One of expected role of intracoronary imaging is the prediction of future cardiovascular events. Current available studies regarding the prediction of future cardiovascular events are summarized as follows and in the *Table 1*.

Grayscale IVUS

There is limited evidence showing the association of

Table 1 Features of intravascular imaging modalities

Features	Grayscale IVUS	VH-IVUS	OCT	NIRS	Angioscopy
Axial resolution	150 μm	200 μm	10-20 μm	N/A	<150 μm
Studies regarding the prediction of cardiovascular events	Echolucent plaque is at risk for ACS (75) Higher plaque burden is associated with MACE (76)	Minimal lumen area of <4 mm^2, plaque burden >70% and VH-derived TCFA predicts ACS (77) VH-derived TCFA predicts MACE (78)	No available evidence exists	Lipid core burden index (LCBI) >43.0 is at risk of MACE (79)	Yellow plaques predict ACS (70) Number of yellow plaques predicts ACS (80) In-stent yellow plaque is at risk of MACE (81)
Advantages	Precise tomographic measurement of lumen area, plaque size and distribution	Ability to differentiate plaque composition	Excellent axial resolution Ability to assess fibrous cap thickness and macrophage filtration	High sensitivity and specificity in the detection of lipid rich plaque	Direct visualization of plaque color and morphology of coronary surface
Disadvantages	Limited axial resolution Inaccuracy in the assessment of plaque composition	Limited axial resolution Inability in the assessment of plaque composition behind calcium	Low tissue penetration Need of contrast medium flush for image acquisition	Lack of prospective data	Need of continuous injection of saline during image acquisition Limited ability to penetrate beyond the coronary surface

IVUS, intravascular ultrasound; VH-IVUS, virtual histology intravascular ultrasound; OCT, optical coherence tomography; NIRS, near infrared spectroscopy; ACS, acute coronary syndrome; MACE, major cardiovascular events.

echolucent plaques with subsequent ACS events. Yamagishi *et al*. has demonstrated that echolucent plaques within non-culprit segments were more likely to develop ACS during follow-up period (75). Another study analyzing IVUS data of 4,137 patients with CAD has reported that baseline plaque burden and its progression rate were associates with major adverse cardiovascular events (76). Clinical outcome in patients having grayscale IVUS derived plaque phenotypes requires further investigation.

Virtual histology intravascular ultrasound (VH-IVUS)

The Providing Regional Observations to Study Predictors of Events in Coronary Tree (PROSPECT) trial, used angiography, three-vessel grayscale and VH-IVUS to evaluate the natural history of atherosclerosis in a 697 patients with ACS. This study has demonstrated that minimal luminal area of <4 mm^2, a plaque burden of >70%, and VH-IVUS derived TCFA were independent determinants of future adverse cardiac events in non-culprit lesions (77). Another study also elucidated TCFA on VH-IVUS was associated with cardiovascular events in 170 patients with stable angina or ACS requiring PCI (78).

Optical coherence tomography (OCT)

Currently, there is no study demonstrating that high-risk plaques on OCT predict future cardiovascular events. One of reasons is the lack of large-scale study to elucidate predictive ability of OCT imaging in cardiovascular events. Specific OCT-derived plaque features associated with clinical outcomes might not be fully evaluated. There are still needs to validate the significance of plaque microstructures on OCT imaging.

Near-infrared spectroscopy (NIRS)

Oemrawsingh *et al*. has recently reported that LCBI predicts future cardiovascular events in patients with CAD. In this study, LCBI above 43.0 within non-culprit arteries had a 4-fold risk of major adverse cardiovascular events in 203 patients during 1-year follow-up (79).

Angioscopy

It has been reported that the presence of yellow plaques was associated with future ACS events (71). The number of yellow plaques has also been shown to predict future ACS events. Evaluation of angioscopic findings in

552 patients has demonstrated number of yellow color plaque as the independent risk factors of ACS events (80). In another study, in-stent yellow plaque at 1-year after stent implantation was associated with higher incidence of major cardiovascular events (81).

Summary and future perspective

The present review describes that (I) various invasive imaging modalities allow to evaluate both plaque burden and composition *in vivo*; (II) plaque imaging provides a unique opportunity to identify vulnerable plaques, elucidate atherosclerotic mechanisms contributing to coronary events and the effect of anti-atherosclerotic medical therapies on coronary atheroma. Although these modalities are considerably promoting our knowledge of coronary atherosclerosis, there remains some limitations regarding axial resolution, penetration and differentiation of plaque composition. Several future directions can be considered to overcome these limitations. Firstly, Improvement in the spatial resolution of conventional modalities may enable more accurate analysis of atherosclerotic plaque. For example, micro OCT has been recently developed and tested in cadaver coronary arteries. As the resolution of this modality is around 10 μm, cellular and subcellular features associated with atherogenesis are clearly imaged (82). Secondly, fusion of different imaging modalities may cover inherent limitation of each modality (83). Combined system of NIRS and IVUS is one of examples enabling to analyze both vessel structure and plaque composition simultaneously. Given that IVUS has limited ability in evaluating plaque composition and NIRS does not provide measurers of vessel wall, combination of NIRS and IVUS helps clinicians to assess both morphological and compositional characteristics of plaques. As such, on-going innovation of technology will be expected to develop novel imaging devices which contain further sophisticated ability to image plaques. Additionally, we have to understand and investigate how these modalities can be used more effectively to manage patients with CAD.

Acknowledgements

None.

Footnote

Conflicts of Interest: Y Kataoka is supported by Cerenis Therapeutics. Other authors have no conflicts of interest to declare.

References

1. Libby P, Ridker PM, Maseri A. Inflammation and atherosclerosis. Circulation 2002;105:1135-43.
2. Libby P. Mechanisms of acute coronary syndromes. N Engl J Med 2013;369:883-4.
3. Nissen SE, Tuzcu EM, Libby P, et al. Effect of antihypertensive agents on cardiovascular events in patients with coronary disease and normal blood pressure: the CAMELOT study: a randomized controlled trial. JAMA 2004;292:2217-25.
4. Okazaki S, Yokoyama T, Miyauchi K, et al. Early statin treatment in patients with acute coronary syndrome: demonstration of the beneficial effect on atherosclerotic lesions by serial volumetric intravascular ultrasound analysis during half a year after coronary event: the ESTABLISH Study. Circulation 2004;110:1061-8.
5. Nissen SE, Nicholls SJ, Sipahi I, et al. Effect of very high-intensity statin therapy on regression of coronary atherosclerosis: the ASTEROID trial. JAMA 2006;295:1556-65.
6. Taylor FC, Huffman M, Ebrahim S. Statin therapy for primary prevention of cardiovascular disease. JAMA 2013;310:2451-2.
7. Tsujita K, Sugiyama S, Sumida H, et al. Impact of Dual Lipid-Lowering Strategy With Ezetimibe and Atorvastatin on Coronary Plaque Regression in Patients With Percutaneous Coronary Intervention: The Multicenter Randomized Controlled PRECISE-IVUS Trial. J Am Coll Cardiol 2015;66:495-507.
8. Nicholls SJ, Ballantyne CM, Barter PJ, et al. Effect of two intensive statin regimens on progression of coronary disease. N Engl J Med 2011;365:2078-87.
9. Pedersen TR, Faergeman O, Kastelein JJ, et al. High-dose atorvastatin vs usual-dose simvastatin for secondary prevention after myocardial infarction: the IDEAL study: a randomized controlled trial. JAMA 2005;294:2437-45.
10. LaRosa JC, Grundy SM, Waters DD, et al. Intensive lipid lowering with atorvastatin in patients with stable coronary disease. N Engl J Med 2005;352:1425-35.
11. Suh WM, Seto AH, Margey RJ, et al. Intravascular detection of the vulnerable plaque. Circ Cardiovasc Imaging 2011;4:169-78.
12. Vancraeynest D, Pasquet A, Roelants V, et al. Imaging the vulnerable plaque. J Am Coll Cardiol 2011;57:1961-79.

13. Nissen SE, Yock P. Intravascular ultrasound: novel pathophysiological insights and current clinical applications. Circulation 2001;103:604-16.
14. Park SJ, Kim YH, Park DW, et al. Impact of intravascular ultrasound guidance on long-term mortality in stenting for unprotected left main coronary artery stenosis. Circ Cardiovasc Interv 2009;2:167-77.
15. Hong YJ, Jeong MH, Choi YH, et al. Impact of plaque components on no-reflow phenomenon after stent deployment in patients with acute coronary syndrome: a virtual histology-intravascular ultrasound analysis. Eur Heart J 2011;32:2059-66.
16. Roy P, Steinberg DH, Sushinsky SJ, et al. The potential clinical utility of intravascular ultrasound guidance in patients undergoing percutaneous coronary intervention with drug-eluting stents. Eur Heart J 2008;29:1851-7.
17. Witzenbichler B, Maehara A, Weisz G, et al. Relationship between intravascular ultrasound guidance and clinical outcomes after drug-eluting stents: the assessment of dual antiplatelet therapy with drug-eluting stents (ADAPT-DES) study. Circulation 2014;129:463-70.
18. Tardif JC, Gregoire J, L'Allier PL, et al. Effects of the acyl coenzyme A:cholesterol acyltransferase inhibitor avasimibe on human atherosclerotic lesions. Circulation 2004;110:3372-7.
19. Nissen SE, Nicholls SJ, Wolski K, et al. Comparison of pioglitazone vs glimepiride on progression of coronary atherosclerosis in patients with type 2 diabetes: the PERISCOPE randomized controlled trial. JAMA 2008;299:1561-73.
20. Hartmann M, Huisman J, Bose D, et al. Serial intravascular ultrasound assessment of changes in coronary atherosclerotic plaque dimensions and composition: an update. Eur J Echocardiogr 2011;12:313-21.
21. Mintz GS, Nissen SE, Anderson WD, et al. American College of Cardiology Clinical Expert Consensus Document on Standards for Acquisition, Measurement and Reporting of Intravascular Ultrasound Studies (IVUS). A report of the American College of Cardiology Task Force on Clinical Expert Consensus Documents. J Am Coll Cardiol 2001;37:1478-92.
22. Pu J, Mintz GS, Biro S, et al. Insights into echo-attenuated plaques, echolucent plaques, and plaques with spotty calcification: novel findings from comparisons among intravascular ultrasound, near-infrared spectroscopy, and pathological histology in 2,294 human coronary artery segments. J Am Coll Cardiol 2014;63:2220-33.
23. Okura H, Taguchi H, Kubo T, et al. Atherosclerotic plaque with ultrasonic attenuation affects coronary reflow and infarct size in patients with acute coronary syndrome: an intravascular ultrasound study. Circ J 2007;71:648-53.
24. Lee SY, Mintz GS, Kim SY, et al. Attenuated plaque detected by intravascular ultrasound: clinical, angiographic, and morphologic features and post-percutaneous coronary intervention complications in patients with acute coronary syndromes. JACC Cardiovasc Interv 2009;2:65-72.
25. Wu X, Mintz GS, Xu K, et al. The relationship between attenuated plaque identified by intravascular ultrasound and no-reflow after stenting in acute myocardial infarction: the HORIZONS-AMI (Harmonizing Outcomes With Revascularization and Stents in Acute Myocardial Infarction) trial. JACC Cardiovasc Interv 2011;4:495-502.
26. Schoenhagen P, Ziada KM, Kapadia SR, et al. Extent and direction of arterial remodeling in stable versus unstable coronary syndromes: an intravascular ultrasound study. Circulation 2000;101:598-603.
27. Hodgson JM, Reddy KG, Suneja R, et al. Intracoronary ultrasound imaging: correlation of plaque morphology with angiography, clinical syndrome and procedural results in patients undergoing coronary angioplasty. J Am Coll Cardiol 1993;21:35-44.
28. Rasheed Q, Nair R, Sheehan H, et al. Correlation of intracoronary ultrasound plaque characteristics in atherosclerotic coronary artery disease patients with clinical variables. Am J Cardiol 1994;73:753-8.
29. Pu J, Mintz GS, Brilakis ES, et al. In vivo characterization of coronary plaques: novel findings from comparing greyscale and virtual histology intravascular ultrasound and near-infrared spectroscopy. Eur Heart J 2012;33:372-83.
30. Fukuda D, Kawarabayashi T, Tanaka A, et al. Lesion characteristics of acute myocardial infarction: an investigation with intravascular ultrasound. Heart 2001;85:402-6.
31. Virmani R, Kolodgie FD, Burke AP, et al. Lessons from sudden coronary death: a comprehensive morphological classification scheme for atherosclerotic lesions. Arterioscler Thromb Vasc Biol 2000;20:1262-75.
32. Otsuka F, Joner M, Prati F, et al. Clinical classification of plaque morphology in coronary disease. Nat Rev Cardiol 2014;11:379-89.
33. Lee JB, Mintz GS, Lisauskas JB, et al. Histopathologic validation of the intravascular ultrasound diagnosis of calcified coronary artery nodules. Am J Cardiol 2011;108:1547-51.
34. Xu Y, Mintz GS, Tam A, et al. Prevalence, distribution, predictors, and outcomes of patients with calcified nodules

in native coronary arteries: a 3-vessel intravascular ultrasound analysis from Providing Regional Observations to Study Predictors of Events in the Coronary Tree (PROSPECT). Circulation 2012;126:537-45.
35. Burke AP, Weber DK, Kolodgie FD, et al. Pathophysiology of calcium deposition in coronary arteries. Herz 2001;26:239-44.
36. Kolodgie FD, Burke AP, Farb A, et al. The thin-cap fibroatheroma: a type of vulnerable plaque: the major precursor lesion to acute coronary syndromes. Curr Opin Cardiol 2001;16:285-92.
37. Ehara S, Kobayashi Y, Yoshiyama M, et al. Spotty calcification typifies the culprit plaque in patients with acute myocardial infarction: an intravascular ultrasound study. Circulation 2004;110:3424-9.
38. Kataoka Y, Wolski K, Uno K, et al. Spotty calcification as a marker of accelerated progression of coronary atherosclerosis: insights from serial intravascular ultrasound. J Am Coll Cardiol 2012;59:1592-7.
39. Matsuo Y, Cassar A, Li J, et al. Repeated episodes of thrombosis as a potential mechanism of plaque progression in cardiac allograft vasculopathy. Eur Heart J 2013;34:2905-15.
40. Nasu K, Tsuchikane E, Katoh O, et al. Accuracy of in vivo coronary plaque morphology assessment: a validation study of in vivo virtual histology compared with in vitro histopathology. J Am Coll Cardiol 2006;47:2405-12.
41. Nair A, Kuban BD, Tuzcu EM, et al. Coronary plaque classification with intravascular ultrasound radiofrequency data analysis. Circulation 2002;106:2200-6.
42. Kolodgie FD, Burke AP, Nakazawa G, et al. Is pathologic intimal thickening the key to understanding early plaque progression in human atherosclerotic disease? Arterioscler Thromb Vasc Biol 2007;27:986-9.
43. Garcia-Garcia HM, Costa MA, Serruys PW. Imaging of coronary atherosclerosis: intravascular ultrasound. Eur Heart J 2010;31:2456-69.
44. García-García HM, Mintz GS, Lerman A, et al. Tissue characterisation using intravascular radiofrequency data analysis: recommendations for acquisition, analysis, interpretation and reporting. EuroIntervention 2009;5:177-89.
45. Burke AP, Farb A, Malcom GT, et al. Coronary risk factors and plaque morphology in men with coronary disease who died suddenly. N Engl J Med 1997;336:1276-82.
46. Thim T, Hagensen MK, Wallace-Bradley D, et al. Unreliable assessment of necrotic core by virtual histology intravascular ultrasound in porcine coronary artery disease. Circ Cardiovasc Imaging 2010;3:384-91.
47. Kawasaki M, Bouma BE, Bressner J, et al. Diagnostic accuracy of optical coherence tomography and integrated backscatter intravascular ultrasound images for tissue characterization of human coronary plaques. J Am Coll Cardiol 2006;48:81-8.
48. Sathyanarayana S, Carlier S, Li W, et al. Characterisation of atherosclerotic plaque by spectral similarity of radiofrequency intravascular ultrasound signals. EuroIntervention 2009;5:133-9.
49. Kume T, Akasaka T, Kawamoto T, et al. Measurement of the thickness of the fibrous cap by optical coherence tomography. Am Heart J 2006;152:755.e1-4.
50. Moreno PR, Falk E, Palacios IF, et al. Macrophage infiltration in acute coronary syndromes. Implications for plaque rupture. Circulation 1994;90:775-8.
51. Kitabata H, Tanaka A, Kubo T, et al. Relation of microchannel structure identified by optical coherence tomography to plaque vulnerability in patients with coronary artery disease. Am J Cardiol 2010;105:1673-8.
52. Uemura S, Ishigami K, Soeda T, et al. Thin-cap fibroatheroma and microchannel findings in optical coherence tomography correlate with subsequent progression of coronary atheromatous plaques. Eur Heart J 2012;33:78-85.
53. Kataoka Y, Puri R, Hammadah M, et al. Cholesterol crystals associate with coronary plaque vulnerability in vivo. J Am Coll Cardiol 2015;65:630-2.
54. Romero ME, Yahagi K, Kolodgie FD, et al. Neoatherosclerosis From a Pathologist's Point of View. Arterioscler Thromb Vasc Biol 2015;35:e43-9.
55. Inoue K, Abe K, Ando K, et al. Pathological analyses of long-term intracoronary Palmaz-Schatz stenting; Is its efficacy permanent? Cardiovasc Pathol 2004;13:109-15.
56. Habara M, Terashima M, Suzuki T. Detection of atherosclerotic progression with rupture of degenerated in-stent intima five years after bare-metal stent implantation using optical coherence tomography. J Invasive Cardiol 2009;21:552-3.
57. Kang SJ, Mintz GS, Akasaka T, et al. Optical coherence tomographic analysis of in-stent neoatherosclerosis after drug-eluting stent implantation. Circulation 2011;123:2954-63.
58. Yonetsu T, Kim JS, Kato K, et al. Comparison of incidence and time course of neoatherosclerosis between bare metal stents and drug-eluting stents using optical coherence tomography. Am J Cardiol 2012;110:933-9.
59. Nakazawa G, Otsuka F, Nakano M, et al. The pathology of

neoatherosclerosis in human coronary implants bare-metal and drug-eluting stents. J Am Coll Cardiol 2011;57:1314-22.
60. Otsuka F, Byrne RA, Yahagi K, et al. Neoatherosclerosis: overview of histopathologic findings and implications for intravascular imaging assessment. Eur Heart J 2015;36:2147-59.
61. Amabile N, Souteyrand G, Ghostine S, et al. Very late stent thrombosis related to incomplete neointimal coverage or neoatherosclerotic plaque rupture identified by optical coherence tomography imaging. Eur Heart J Cardiovasc Imaging 2014;15:24-31.
62. Takano M, Yamamoto M, Inami S, et al. Appearance of lipid-laden intima and neovascularization after implantation of bare-metal stents extended late-phase observation by intracoronary optical coherence tomography. J Am Coll Cardiol 2009;55:26-32.
63. Wang J, Geng YJ, Guo B, et al. Near-infrared spectroscopic characterization of human advanced atherosclerotic plaques. J Am Coll Cardiol 2002;39:1305-13.
64. Kang SJ, Mintz GS, Pu J, et al. Combined IVUS and NIRS detection of fibroatheromas: histopathological validation in human coronary arteries. JACC Cardiovasc Imaging 2015;8:184-94.
65. Cassis LA, Lodder RA. Near-IR imaging of atheromas in living arterial tissue. Anal Chem 1993;65:1247-56.
66. Madder RD, Goldstein JA, Madden SP, et al. Detection by near-infrared spectroscopy of large lipid core plaques at culprit sites in patients with acute ST-segment elevation myocardial infarction. JACC Cardiovasc Interv 2013;6:838-46.
67. Puri R, Madder RD, Madden SP, et al. Near-Infrared Spectroscopy Enhances Intravascular Ultrasound Assessment of Vulnerable Coronary Plaque: A Combined Pathological and In Vivo Study. Arterioscler Thromb Vasc Biol 2015;35:2423-31.
68. Raghunathan D, Abdel-Karim AR, Papayannis AC, et al. Relation between the presence and extent of coronary lipid core plaques detected by near-infrared spectroscopy with postpercutaneous coronary intervention myocardial infarction. Am J Cardiol 2011;107:1613-8.
69. Goldstein JA, Maini B, Dixon SR, et al. Detection of lipid-core plaques by intracoronary near-infrared spectroscopy identifies high risk of periprocedural myocardial infarction. Circ Cardiovasc Interv 2011;4:429-37.
70. Kubo T, Imanishi T, Takarada S, et al. Implication of plaque color classification for assessing plaque vulnerability: a coronary angioscopy and optical coherence tomography investigation. JACC Cardiovasc Interv 2008;1:74-80.
71. Uchida Y, Nakamura F, Tomaru T, et al. Prediction of acute coronary syndromes by percutaneous coronary angioscopy in patients with stable angina. Am Heart J.1995;130:195-203.
72. Waxman S, Sassower MA, Mittleman MA, et al. Angioscopic predictors of early adverse outcome after coronary angioplasty in patients with unstable angina and non-Q-wave myocardial infarction. Circulation 1996;93:2106-13.
73. Siegel RJ, Ariani M, Fishbein MC, et al. Histopathologic validation of angioscopy and intravascular ultrasound. Circulation 1991;84:109-17.
74. Maeng M, den Heijer P, Olesen PG, et al. Histopathologic validation of in-vivo angioscopic observation of coronary thrombus after angioplasty in a porcine model. Coron Artery Dis 2001;12:53-9.
75. Yamagishi M, Terashima M, Awano K, et al. Morphology of vulnerable coronary plaque: insights from follow-up of patients examined by intravascular ultrasound before an acute coronary syndrome. J Am Coll Cardiol 2000;35:106-11.
76. Nicholls SJ, Hsu A, Wolski K, et al. Intravascular ultrasound-derived measures of coronary atherosclerotic plaque burden and clinical outcome. J Am Coll Cardiol 2010;55:2399-407.
77. Stone GW, Maehara A, Lansky AJ, et al. A prospective natural-history study of coronary atherosclerosis. N Engl J Med 2011;364:226-35.
78. Calvert PA, Obaid DR, O'Sullivan M, et al. Association between IVUS findings and adverse outcomes in patients with coronary artery disease: the VIVA (VH-IVUS in Vulnerable Atherosclerosis) Study. JACC Cardiovasc Imaging 2011;4:894-901.
79. Oemrawsingh RM, Cheng JM, Garcia-Garcia HM, et al. Near-infrared spectroscopy predicts cardiovascular outcome in patients with coronary artery disease. J Am Coll Cardiol 2014;64:2510-8.
80. Ohtani T, Ueda Y, Mizote I, et al. Number of yellow plaques detected in a coronary artery is associated with future risk of acute coronary syndrome: detection of vulnerable patients by angioscopy. J Am Coll Cardiol 2006;47:2194-200.
81. Ueda Y, Matsuo K, Nishimoto Y, et al. In-Stent Yellow Plaque at 1 Year After Implantation Is Associated With Future Event of Very Late Stent Failure: The DESNOTE Study (Detect the Event of Very late Stent Failure From the Drug-Eluting Stent Not Well Covered by Neointima Determined by Angioscopy). JACC Cardiovasc Interv

2015;8:814-21.
82. Liu L, Gardecki JA, Nadkarni SK, et al. Imaging the subcellular structure of human coronary atherosclerosis using micro-optical coherence tomography. Nat Med 2011;17:1010-4.
83. Bourantas CV, Garcia-Garcia HM, Naka KK, et al. Hybrid intravascular imaging: current applications and prospective potential in the study of coronary atherosclerosis. J Am Coll Cardiol 2013;61:1369-78.

Cite this article as: Honda S, Kataoka Y, Kanaya T, Noguchi T, Ogawa H, Yasuda S. Characterization of coronary atherosclerosis by intravascular imaging modalities. Cardiovasc Diagn Ther 2016;6(4):368-381. doi: 10.21037/cdt.2015.12.05

